INFORMAL COMMENTARIES ON THE NUMERICAL INVESTIGATION OF THE "TOY MODEL" [H. BIRKELAND – J.-C.Y. – ORSAY – SEPT. 98]

JEAN-CHRISTOPHE YOCCOZ

Recall that the toy model is given by

$$(*) \quad N(t) = \int_{A_0}^{A_1} S(a)N(t-a)m_\rho(t-a)m(N(t-a))da$$

where t is time and

- N is the active population, with age $\geqslant A_0$;
- A_1 is the maximal age;
- A_0 is the maturation age;
- S is the survival rate; we take $S(a) = 1 - \frac{a}{A_1}$.
- $m_\rho(t)$ is the seasonal parameter: time is counted in years; with $0 \leqslant \rho \leqslant 1$, one has $m_\rho(t) = \left\{ \begin{array}{ll} 0 & \text{if } 0 \leqslant t \leqslant \rho \\ 1 & \text{if } \rho \leqslant t \leqslant 1 \end{array} \right\}$ mod 1
  [ρ is the length of the winter]
- $m(N)$ is the fecundity rate at (active) population N: we take it of the form

$$m(N) = \left\{ \begin{array}{ll} m_0 & \text{if } N \leqslant 1 \\ m_0 N^{-\gamma} & \text{if } N \geqslant 1 \end{array} \right.$$

The model thus depends on five parameters A_0, A_1, ρ, m_0, γ. We took always $A_1 = 2$, and most of the time we took $m_0 = 50$. Our findings suggest (see commentary later) that it would be worth investigating slightly lower values of m_0.

1. UNSEASONAL MODEL: $\rho = 0$

(a) We have then an equilibrium (constant solution) at

$$N_{eq} = \left[m_0 \frac{A_1}{2} \left(1 - \frac{A_0}{A_1} \right)^2 \right]^{1/\gamma}$$

provided this quantity is > 1 [it is so for any reasonable value of the parameters]. Defining [see text October 1997][1]

$$\begin{aligned} F(\lambda) &= \int_{A_0}^{A_1} S(a)e^{-a\lambda}da \\ &= \left(\frac{1}{\lambda}(1 - \frac{A_0}{A_1}) - \frac{1}{\lambda^2 A_1} \right) e^{-A_0\lambda} + \frac{1}{\lambda^2 A_1} e^{-A_1\lambda} \end{aligned}$$

[0]The original manuscript was converted into 'tex' by Sylvain Arlot and Carlos Matheus. Up to some minor modifications, this article is faithful to the original text.

[1]Here and in what follows, "Oct. 97" is a reference to the text *The numerical toy model* by Jean-Christophe Yoccoz (available at the website dedicated to his mathematical archives, for instance).

the eigenvalues at the equilibrium are the complex numbers λ solutions of

$$F(\lambda) = \frac{A_1}{2}\left(1 - \frac{A_0}{A_1}\right)^2 (1-\gamma)^{-1} := c_\gamma$$

[Observe that provided $N_{eq} > 1$, the parameter m_0 *does not* enter in the discussion of the eigenvalues, and in particular of the stability of the equilibrium]. One expects that (for reasonable values of A_0) [see Oct. 1997]:

- the zeroes of the equation

$$\mathrm{Im} F(-iu) = 0, \quad u > 0$$

(where $F(-iu) = u^{-1}(1 - \frac{A_0}{A_1})\cos A_0 u + u^{-2}A_1^{-1}(\sin A_0 u - \sin A_1 u)$) for $u_0 < u_1 < u_2 < \dots$ with

$$\begin{cases} \text{Re } F(-i\,u_{2k}) < \text{Re } F(-i\,u_{2k+2}) < 0 \\ \text{Re } F(-i\,u_{2k+1}) > \text{Re } F(-i\,u_{2k+3}) > 0 \end{cases}$$

[this is easily proved for large k; for the first values of k, one needs a direct computation].

We checked that this is true for several significant values of A_0.

We also computed the values $u_0 = u_0(A_0), u_2 = u_2(A_0), \dots$ Then we know that

- if $\gamma < 1 + \frac{A_1}{2}(1 - \frac{A_0}{A_1})^2 |F(-iu_0)|^{-1} := \gamma_0(A_0)$ the equilibrium is stable.
- if $\gamma_0(A_0) < \gamma < 1 + \frac{A_1}{2}(1 - \frac{A_0}{A_1})^2 |F(-iu_2)|^{-1} := \gamma_1(A_0)$ there are exactly two (complex conjugate) unstable eigenvalues
- if $\gamma_{k-1}(A_0) < \gamma < 1 + \frac{A_1}{2}(1 - \frac{A_0}{A_1})^2 |F(-iu_{2k})|^{-1} := \gamma_k(A_0)$ there are exactly $2k$ unstable eigenvalues (k pairs of complex conjugates).

Actually, $\gamma_0, \gamma_1, \dots$ do not depend much on A_0; a typical value for γ_0 is ~ 6.2, a typical value for γ_1 is ~ 30.

As γ increase through γ_0 (for fixed A_0), one expects a *Hopf bifurcation* (see Appendix B): an attracting periodic orbit is born at the equilibrium (for $\gamma = \gamma_0$) and attracts all solutions near the equilibrium for $\gamma > \gamma_0$ (close to γ_0) [except the equilibrium itself].

Remark 1.1. With some easy work, everything in this section could be proved in a completely rigorous way.

(b) For $\gamma > \gamma_0(A_0)$ ($\simeq 6.2$), the equilibrium is no more stable and the attention switches to the stable periodic orbit born from the equilibrium at $\gamma = \gamma_0$.

We followed numerically this periodic orbit for increasing values of γ (A_0 being fixed).

Around $\gamma \sim 8.2$, it seems that the periodic orbit loses its stability: the numerical evidence is that we have for some critical value γ_0' of γ a *Hopf bifurcation* (for a periodic orbit, see *Appendix* C) giving rise for $\gamma > \gamma_0'$ to *quasiperiodic motion*; the quasiperiodic orbits should fill a 2-dimensional torus in ∞-dimensional phase space, and we were able to "vizualize" this torus [cf. representation $[N(t), N(t+1), N(t+2)]$ explained later on].

Remark 1.2. The mathematical theory of the Hopf bifurcation is easy, but to check *rigorously* that the conditions for it to occur are satisfied in our case would probably require some painful work.

(c) For $0 < \gamma < 2$, it is easy to *prove* that *all* solutions are attracted by the stable equilibrium.

For $\gamma < \gamma_0$ ($\simeq 6.2$), this is still true for all solutions *near* the equilibrium.

However, we *did observe* some stable periodic orbits *far from the equilibrium* for certain values of γ (~ 4) with $\gamma_0 > \gamma > 2$.

Following these stable periodic orbits for increasing values of γ, they persist till some rather large value of γ and then disappear.

Both the birth and the death of this "large" periodic orbits could be explained by *saddle-node bifurcations* (see Appendix D).

2. THE SEASONAL MODEL: CHAOTIC ATTRACTORS

With four parameters to play with $[m_0, A_0, \rho, \gamma]$, a systematic exploration of the parameter space is hopeless. After some educated guesses, we found two sets of parameter values which exhibit extremely interesting dynamics in an open region of phase space.

In both cases, the stationary regime seems to be a *low-dimensional non-uniformly hyperbolic attractor* [see Appendix E] but the geometry of the phase space involved seems to be rather different in one case and the other.

The two sets of parameter values are:

STRANGE ATTRACTOR I

$A_0 = 0.23$ [$A_1 = 2$], $m_0 = 50$, $\gamma = 8$, $\rho = 0.34$

HENON-LIKE ATTRACTOR II

$A_0 = 0.18$ [$A_1 = 2$], $m_0 = 50$, $\gamma = 8.25$, $\rho = 0.41$
[we get something similar with $A_0 = 0.15$]

2.1. VISUALIZING THE ATTRACTOR(S): THE $N(t), N(t+1), N(t+2)$ REPRESENTATION.

First let me correct a slight (unimportant) mistake in [Oct. 97].

In the seasonal model, the phase space is not the product $Y \times \mathbb{R}/\mathbb{Z}$ as stated there: indeed the condition

$$\oplus_{t_0} : \quad \widetilde{N}(0) = \int_{A_0}^{A_1} S(a)\widetilde{N}(-a)m(\widetilde{N}(-a))m_\rho(t_0 - a)\, da$$

depends on t_0 (mod 1) and defines an hypersurface Y_{t_0} (i.e. codimension 1) of the space C of continuous functions $\widetilde{N}$ on $[-A_1, 0]$ taking positive values.

The phase space is

$$Y^\sharp = \{(t, \widetilde{N}), t \in \mathbb{R}/\mathbb{Z}, \widetilde{N} \in Y_t\}$$

(it is not quite a product). The dynamics $(T^s)_{s \geqslant 0}$ are still given by the semigroup law $T^s \circ T^{s'} = T^{s+s'}$ and

$$T^s(t, \widetilde{N}) = (t + s(\text{mod } 1), \widetilde{N}^s)$$

where, for $0 \leqslant s \leqslant A_0$, we have:

$$\begin{cases} \widetilde{N}^s(-a) = \widetilde{N}(s-a) & \text{if } 0 \leqslant s \leqslant a \leqslant A_1 \\ \widetilde{N}^s(-a) = \int_{A_0}^{A_1} S(b)\widetilde{N}(s-a-b)m(\widetilde{N}(s-a-b))m_\rho(t+s-a-b)\, db & \text{if } 0 \leqslant a \leqslant s \end{cases}$$

Anyway, we want to look at the map

$$T^1 : Y_0 \to Y_0$$

(we could also consider $T^1 : Y_{t_0} \to Y_{t_0}$ which gives essentially the "same" dynamics).

As explained in Appendix F, there is a compact subset $\mathcal{K}_0$ of Y_0 such that

(i) $T^1(\mathcal{K}_0) \subset \mathcal{K}_0$
(ii) for any $N \in Y_0$, we have $T^k(N) \subset \mathcal{K}_0$ for all large k.

We then define the *attractor*

$$\Lambda_0 = \bigcap_{n \geqslant 0} T^n(\mathcal{K}_0)$$

with the following properties

(iii) $T^1(\Lambda_0) = \Lambda_0$; Λ_0 is compact;
(iv) for any $N \in Y_0$, the distance of $T^k(N)$ to Λ_0 goes to zero as k goes to ∞.

Both $\Lambda_0, \mathcal{K}_0$ are compact subsets of the metric space Y_0, the distance being the uniform norm

$$\|N - N'\| = \max_{-A_1 \leqslant s \leqslant 0} |N(s) - N'(s)|$$

The good thing with compact sets is that they can be approximated by finite sets: for any $\varepsilon > 0$, there exist finite ε-dense subsets R, meaning that any point in the compact set is at distance $< \varepsilon$ from a point in R.

Denote by $r(\varepsilon)$ the minimal cardinality of such a subset R [for a smooth curve we have $r(\varepsilon) \sim \varepsilon^{-1}$, for a smooth surface $r(\varepsilon) \sim \varepsilon^{-2}$, ...]; the fractal dimension of the compact set is

$$\lim \frac{\log r(\varepsilon)}{\log \varepsilon^{-1}}$$

i.e. $r(\varepsilon) \sim \varepsilon^{-\dim}$ [the limit does not always exist; then one takes $\limsup$...]

Now the compact set $\mathcal{K}_0$ is infinite dimensional but on general principles (not explained here) the attractor Λ_0 should have *finite fractal dimension* D_0; then one should be able to *vizualize* it in the following way, using the following

Principle 1. *Let E a (perhaps ∞-dimensional) vector space and $\Lambda \subset E$ a compact subset of finite fractal dimension D. Let k be an integer $> 2D$. Then, for the "general" linear projection $p : E \to \mathbb{R}^k$, the map p is one-to-one on Λ and is a homeomorphism onto its image $p(\Lambda) \subset \mathbb{R}^k$.*

In our case E is a space of continuous functions N on $[-A_1, 0]$; the simplest projections that one can think of have the type

$$N \to (N(s_1), N(s_2), N(s_3), \dots, N(s_k)) \in \mathbb{R}^k$$

where $-A_1 \leqslant s_1 < s_2 < \cdots < s_k \leqslant 0$ are any fixed values. To get an image on the screen, we took $k = 3$, $s_1 = -A_1 = -2$, $s_2 = -1$, $s_3 = 0$.

Let $N \in Y_0$ be an initial condition; the set of limit points of $T^k(N)$, as $k \to +\infty$, is called the ω-limit set of N, denoted by $\omega(N)$; it is compact, invariant under T, and contained in Λ_0 according to (iv) above.

Being slightly optmistic, one could hope (expect?) that the full attractor can actually be written as a *disjoint finite union*

$$\Lambda_0 = \omega(N_1) \sqcup \omega(N_2) \sqcup \cdots \sqcup \omega(N_l)$$

for some appropriate initial conditions $N_1, \dots, N_l$.

Anyway, it is important to understand $\omega(N)$ and the dynamics $T^1 : \omega(N) \to \omega(N)$.

Remark 2.1. For the quasiperiodic motion in the unseasonal case, we expect a 2-dimensional torus in ∞-dimensional phase case; to get an injective projection requires a priori $k = 5$. With $k = 3$ (as we did), what we have seen looks indeed like a torus self-intersecting along some lines ... [as it should]

In the seasonal case, for the two sets of parameter values mentioned above, we were able to find initial conditions N such that, apparently

$$1 < \dim(\omega(N)) < 1.5,$$

meaning that $k = 3$ should give an injective projection allowing to vizualize $p(\omega(N)) \subset \mathbb{R}^3$.

What we did in practice, starting with an appropriate initial condition N on $[-A_1, 0]$, was

1) to compute the corresponding solution $N(t)$, $0 \leqslant t \leqslant t_{\max}$ with $t_{\max} = 1000$ years.
2) to plot, for $50 \leqslant n \leqslant 1000$, n integer, the points

$$X_n = (N(n-2), N(n-1), N(n)) \in \mathbb{R}^3$$

(which are precisely, with $p(N) = (N(-2), N(-1), N(0))$, the points $p(T^n(N))$)

Remark 2.2. one has to start at $n \geqslant 50$ to be reasonably confident that $T^n(N)$ is close to $\omega(N)$.

Remark 2.3. in both cases considered, we discovered that $\omega(N)$ is made of two disjoint pieces $\omega_0(N), \omega_1(N)$ exchanged by T such that

$$T^{2n}(N) \to \omega_0(N)$$

$$T^{2n+1}(N) \to \omega_1(N)$$

[ω_0 corresponding to low densities and ω_1 to high densities]. To plot $p(\omega_0(N))$, it is sufficient to consider X_{2n}, $50 \leqslant 2n \leqslant 1000$.

3) we checked (at least in one case) that the 3-dimensional projection p is OK: we took a small box in $\mathbb{R}^3$ containing 30 points X_{n_i} ($1 \leqslant i \leqslant 30$); for these times n_i, we know that the $N(n_i)$ are close to each other, as are the $N(n_i - 1)$ and $N(n_i - 2)$; we checked that the *functions* $N(n_i - s)$, $-A_1 \leqslant s \leqslant 0$, are actually *uniformly close* (for all $-A_1 \leqslant s \leqslant 0$).
4) We checked (for these same times n_i) a sensibility to initial condition, and a Cantor-like structure in the past, which are typical of chaotic attractors: considering the functions $N(n_i - s)$ ($1 \leqslant i \leqslant 30$), which are uniformly close for $-A_1 \leqslant s \leqslant 0$, we observed that they diverge in a rather uniform way for $s > 0$, while they diverge by "packets" for $s < -A_1$: see the picture by H. Birkeland on the computer.[2]
5) The dynamics is obviously $X_n \to X_{n+1}$ (actually $X_{2n} \to X_{2n+2}$, see Remark 2.3, if we are interested in $\omega_0(N)$); by identifying on the screen the successive X_n, one is able to guess what the map $T^1 : \omega(N) \to \omega(N)$ (or $T^2 : \omega_0(N) \to \omega_0(N)$) should look like [see Appendix E].

[2]Unfortunately, we could not find this picture in Jean-Christophe Yoccoz archives. Nevertheless, Jean-Christophe asked Sylvain Arlot to draw a similar picture which became later Figure 27 at page 48 of Arlot's *mémoire de DEA* (available at https://arxiv.org/abs/1204.0799). For the sake of convenience of the reader, we reproduce this figure here as Figure 1.

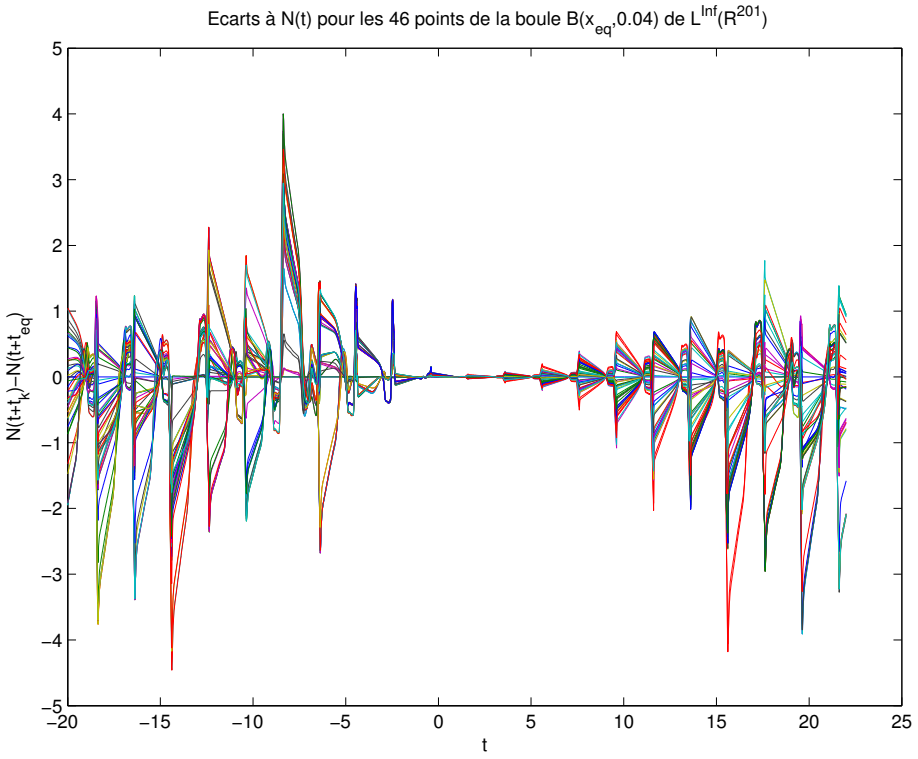

FIGURE 1. S. Arlot's "version" of a picture by H. Birkeland.

3. WHAT'S NEXT?

There are (at least) 3 lines of investigation that suggest themselves

(1) Better understanding of the two chaotic attractors.
(2) Pursuing the investigation of parameter space in the seasonal toy model: there is certainly *much more* to see.
(3) Going to more complicated models, including maternal effects ...

My feeling is that (3) should be postponed till we get a better understanding of the toy model, which serves as a reference.

I will give below some indications for (1) and (2), but there are only general guidelines which should be adapted to what comes out of the simulations!

(1) We fix here one of the two sets of parameter values for which a chaotic attractor was detected.

(a) With 1000-year time series, we have only $\leqslant 500$ points to draw $p(\omega_0(N))$ in $\mathbb{R}^3$. One needs a much longer (50000 to 100000 years) time series ... [and *discard the first* 100 *years, say*]

(b) With say a ~ 30000 pts finite approximation to $\omega_0(N)$ [draw it!]

$$\begin{aligned} X_{2n} &= (N(2n-2), N(2n-1), N(2n)) \\ &= (X^0_{2n}, X^1_{2n}, X^2_{2n}) \end{aligned}$$

located in a box B^0:

$$\begin{aligned} X^0_{\min} \leqslant X^0 \leqslant X^0_{\max} = X^0_{\min} + \Delta X^0 \\ X^1_{\min} \leqslant X^1 \leqslant X^1_{\max} = X^1_{\min} + \Delta X^1 \\ X^2_{\min} \leqslant X^2 \leqslant X^2_{\max} = X^2_{\min} + \Delta X^2 \end{aligned}$$

one can do the following procedure

- divide B^0 in 8 boxes B^1_i ($1 \leqslant i \leqslant 8$) with sides $\frac{1}{2}\Delta X^0$, $\frac{1}{2}\Delta X^1$, $\frac{1}{2}\Delta X^2$; discard those boxes which do not contain any X_{2n}
- for each box B^1_i which is left, divide it into 8 boxes $B^2_{i,j}$ with sides $\frac{1}{4}\Delta X^0$, $\frac{1}{4}\Delta X^1$, $\frac{1}{4}\Delta X^2$; discard those which do *not* contain any X_{2n}

$$\vdots$$

- for each box $B^k_{i_1 \ldots i_k}$ (with sides $2^{-k}\Delta X^0$, $2^{-k}\Delta X^1$, $2^{-k}\Delta X^2$) which is left, divide it into 8 boxes $B^{k+1}_{i_1 \ldots i_{k+1}}$ of sides $2^{-k-1}\Delta X^0$, $2^{-k-1}\Delta X^1$, $2^{-k-1}\Delta X^2$ and discard those which do *not* contain any X_{2n}
- Stop this process at the first integer k_0 for which the number of boxes B^{k_0} which contain some X_{2n} is $\geqslant 3000$.

(c) *Fractal dimension*:

For $0 \leqslant k \leqslant k_0$, let r_k be the number of boxes $B^k_{i_1 \ldots i_k}$ at generation k which contain some X_{2n}. Compute, for $\underline{\frac{k_0}{2} \leqslant k \leqslant k_0}$ (say) the points

$$(k \log 2, \log r_k)$$

They should (!?!) be more or less on a line, the slope of which would be the *fractal dimension of the attractor*.

[with $r_{k_0} \sim 3000$ one can perhaps (??) expect $k_0 \simeq 9$ or 10 and thus get ~ 5 points to draw the line!]

(d) "*Lyapunov exponents*"

- Consider only those boxes $B^{k_0}_{i_1 \ldots i_{k_0}}$ of the k_0^{th} generation which contain at least 10 (say) points;
- for every such box, let $X_{2n_1}, \ldots, X_{2n_r}$ the corresponding points (thus $r \geqslant 10$);
- for $1 \leqslant i < j \leqslant r$, compute

$$D(i,j) = \max_{-2 \leqslant t \leqslant 0} |N(2n_i + t) - N(2n_j + t)|$$

$$D^+(i,j) = \max_{0 \leqslant t \leqslant 2} |N(2n_i + t) - N(2n_j + t)|$$

$$D^-(i,j) = \max_{-4 \leqslant t \leqslant -2} |N(2n_i + t) - N(2n_j + t)|$$

[t is here a "continuous" variable, meaning 240 "steps" if one uses 120 steps/year]

- Compute

$$\lambda^+(i,j) = \frac{D^+(i,j)}{D(i,j)}$$

$$\lambda^-(i,j) = \frac{D^-(i,j)}{D(i,j)}$$

- For the box $B = B^{k_0}_{i_1 \dots i_{k_0}}$ which is considered, define

$$\lambda^+(B) = \max_{1 \leqslant i < j \leqslant r} \lambda^+(i,j)$$

$$\lambda^-(B) = \max_{1 \leqslant i < j \leqslant r} \lambda^-(i,j)$$

- Color the box B (in the 3-D representation) according to the value of $\lambda^+(B)$
- Do the same with $\lambda^-(B)$
- Do the same with the *product* $\lambda^+(B)\lambda^-(B)$
- It would be good to do the same as above with the relative distances:

$$\widehat{D}(i,j) = \max_{-2 \leqslant t \leqslant 0} \left| \frac{N(2n_i + t) - N(2n_j + t)}{N(2n_i + t)} \right|$$

  defining similarly $\widehat{D}^+(i,j), \widehat{D}^-(i,j), \widehat{\lambda}(i,j) = \frac{\widehat{D}^+(i,j)}{\widehat{D}^-(i,j)}, \widehat{\lambda}^-(i,j), \widehat{\lambda}^+(B), \widehat{\lambda}^-(B)$, ... and to compare the pictures.

(e) Checking the geometry of the attractors.

A possible geometry is suggested at the end of Appendix E; I need to think more on the ways that one could check that the guess is right.

(2) *Exploring parameter space*

Keeping $A_1 = 2$, we have still 4 parameters m_0, γ, ρ, A_0 so no systematic exploration is possible.

(a) "Transition to chaos" [we keep here $m_0 = 50$]

Consider the two sets of parameter values

$$P_I = (A_0 = 0.23 \quad \rho = 0.34 \quad \gamma = 8)$$

$$P_{II} = (A_0 = 0.18 \quad \rho = 0.41 \quad \gamma = 8.25)$$

for which a chaotic attractor was observed.

Choose a third set of parameter values, with $\rho = 0$ (unseasonal model) for which we have a stable equilibrium. For instance

$$P_{III} = (A_0 = 0.1, \rho = 0, \gamma = 6)$$

should do (If not take γ slightly smaller).

One wants to let the parameters vary *slowly* along the 3 *lines* which join these three points in parameter space. [50 pts per line should be OK]

What we want to know, for each set of parameter values is

- whether the solution is periodic, and, if yes, which is the period?
- when it is not periodic, what the "attractor" looks like?

One could (!?) proceed as follows (there may be better ways)

- for each new parameter, choose *carefully* the initial data (see below)
- let it run for 50 years (say); draw the points $X_n = (N(n-2), N(n-1), N(n))$ for $10 < n \leqslant 50$
- if it seems that we have only a few points on the screen (say $\leqslant 8$), the solution is periodic and the number of points is the period
- otherwise, one should compute the solution for 500 years (say), and look again at the $(X_n)_{50 \leqslant n \leqslant 500}$ ...

Anyway, I feel that one shouldn't have a rigid strategy beforehand ... One should adapt it to the situations encountered.

Remark on initial conditions: For many sets of parameter values, it appears that we have *several* stable stationary regimes, each with its own basin of attraction; therefore the choice of initial conditions *is* important; for instance, for the parameter values giving chaotic attractors, there is also a stable periodic orbit (far from the attractors).

When one tries a set of parameter values *far* from anything tested before, it is difficult to guess a good choice of initial conditions: one should just avoid a *discontinuity* in the solution [see the modification we did by affine interpolation on $[-A_0, 0]$].

On the other hand, when we consider a set of parameter values $\widetilde{P}$ *close* to a set P (which has been tested to give something interesting, one could do the following

- choose a first approximation for initial conditions for $\widetilde{P}$, a two-year period of the solution for P for instance $N^0_P(t) = N_P(30+t)$ for $-2 \leqslant t \leqslant 0$.
- this is a reasonable choice, but not completely satisfactory because we have created a small discontinuity at time $t = 0$; indeed, we have

$$N_P(30) = \int_{A_0}^{A_1=2} S(a) m_\rho(30-a) m(N_P(30-a))\, da$$

and therefore

$$|N^0_{\widetilde{P}}(0) - \int_{\widetilde{A}_0}^{A_1=2} S(a) m_{\widetilde{\rho}}(30-a) \widetilde{m}(N^0_{\widetilde{P}}(-a))\, da|$$

(with $\widetilde{\rho}, \widetilde{A}_0, \widetilde{\gamma}, \widetilde{m}_0$ close to ρ, A_0, γ, m_0) is small but non zero. What one could do is to modify $N^0_{\widetilde{P}}$ into $N_{\widetilde{P}}$ on $[-2, 0]$ as follows:

  - compute $N_{\widetilde{P}}(0) = \int_{\widetilde{A}_0}^{A_1=2} S(a) m_{\widetilde{\rho}}(30-a) \widetilde{m}(N_P(30-a))\, da$ (with the *new* set $\widetilde{P}$ of parameter values)
  - define the new set $N_{\widetilde{P}}(t)$ of initial conditions ($-2 \leqslant t \leqslant 0$) as

$$\begin{cases} N_{\widetilde{P}}(t) = N^0_{\widetilde{P}}(t) = N_P(30-a) \text{ for } -2 \leqslant t \leqslant -\widetilde{A}_0 \\ \text{on } -\widetilde{A}_0 \leqslant t \leqslant 0, \text{make the affine } \textit{correction} \\ \text{which makes } N_{\widetilde{P}} \text{ continuous, i.e.} \\ N_{\widetilde{P}}(t) = N^0_{\widetilde{P}}(t) + [N_{\widetilde{P}}(0) - N^0_{\widetilde{P}}(0)] \frac{t+\widetilde{A}_0}{\widetilde{A}_0} \\ = N_P(30+t) + [N_{\widetilde{P}}(0) - N_P(30)] \frac{t+\widetilde{A}_0}{\widetilde{A}_0} \end{cases}$$

This should give a satisfactory set of initial values allowing to "follow"[3] attractors when parameter values change slowly.

Remark 3.1. In the same spirit, when exploring the lines $P_I P_{III}$ or $P_{II} P_{III}$ in parameter space, it is better to *start* from P_I or P_{II}; it is not excluded at all (and perhaps it's worth testing it) that starting from P_{III} (with stable equilibrium), what one gets at P_I or P_{II} is *not* the chaotic attractor but another stable stationary regime that coexists from the *same parameters*.

(b) Plainly the chaotic attractors that we saw do not correspond faithfully to what is observed: there is a succession of high and lows on a 2-year basis [cf. decomposition

[3] In this direction, Sylvain Arlot produced some movies (available at https://hal.inria.fr/hal-00679905/) showing how some attractors change when the parameter A_0 varies.

$\omega(N) = \omega_0(N) \cup \omega_1(N)$] which is too short compared to reality. Also, our parameter values are not quite realistic.

The too short succession of highs and lows could be explained by a too large value of m_0: intuitively, after a crash, the population will increase exponentially fast, till it gets well past the threshold $N = 1$ and crashes again; with m_0 large, the exponential increase is very fast, and it takes short time before the next crash.

Therefore, it seems worthwhile to start from the parameter values giving chaotic attractors, and to change slowly the value of m_0 to lower values ...

On the other hand, I am not too much worried to have slightly unrealistic parameter values for ρ and A_0; on one hand, fecundity is probably not completely 0 in the winter (according to what Nigel[4] told me); on the other, if we find in the toy model the right kind of chaotic dynamics, one could hope to "follow" it in more complicated models (maternal effects!) where it could exist for more realistic parameter values ...

[4]Nigel Gilles Yoccoz.

APPENDIX A. SCALING THE POPULATION IN THE TOY MODEL

(a) *Cut-off at* $N = 1$
We have here

$$(1) \quad N(t) = \int_{A_0}^{A_1} S(a)N(t-a)m_\rho(t-a)m(N(t-a))\,da$$

with

$$m(N) = \begin{cases} m_0 & \text{for } N \leqslant 1 \\ m_0 N^{-\gamma} & \text{for } N \geqslant 1 \end{cases}$$

(b) Let $s > 0$, and let $\widehat{N} = sN$; the equation (1) gives

$$(1_s) \quad \widehat{N}(t) = \int_{A_0}^{A_1} S(a)\widehat{N}(t-a)m_\rho(t-a)m(N(t-a))\,da$$

and writing $m(N) = \widehat{m}(\widehat{N})$, we have

$$\widehat{m}(\widehat{N}) = \begin{cases} m_0 & \text{for } \widehat{N} \leqslant s \\ m_0 s^{-\gamma}\widehat{N}^{-\gamma} & \text{for } \widehat{N} \geqslant s \end{cases}$$

There are two reasonable choices for s (one of which is indicated in the text.

(1) we take $s = m_0^{-1/\gamma}$, which gives $m_0 s^\gamma = 1$; setting $\widehat{N}_c = s$ gives

$$\widehat{m}(\widehat{N}) = \begin{cases} \widehat{N}_c^{-\gamma} & \text{for } \widehat{N} \leqslant \widehat{N}_c \\ \widehat{N}^{-\gamma} & \text{for } \widehat{N} \geqslant \widehat{N}_c \end{cases}$$

(2) If $m_0 \int_{A_0}^{A_1} S(a)\,da > 1$ (which will always be satisfied for reasonable choices of m_0), we take s such that

$$[m_0 \int_{A_0}^{A_1} S(a)\,da]s^\gamma = 1;$$

the *equilibrium* in the *unseasonal* case is at $N = s^{-1}$, i.e. $\underline{\widehat{N} = 1}$.

We then have

$$\widehat{m}(\widehat{N}) = \begin{cases} m_0 & \text{for } \widehat{N} \leqslant \widehat{N}_c^1 \\ (\int_{A_0}^{A_1} S(a)\,da)^{-1}\widehat{N}^{-\gamma} & \text{for } \widehat{N} \geqslant \widehat{N}_c^1 \end{cases}$$

where

$$\widehat{N}_c^1 = s = \left(m_0 \int_{A_0}^{A_1} S(a)\,da\right)^{-1/\gamma}$$

Going from the scale (a) (variable N) to scales (b1) or (b2) involves a change of scale which *depends* on the cutoff level m_0; on the other hand, the change of scales from (b1) to (b2) depends not on m_0, but *only* on the function S (which is *fixed*).

APPENDIX B. HOPF BIFURCATION FOR EQUILIBRIA

B.1. **Model in the plane.** Consider the 1-parameter family of differential equations in the plane

$$(*_\varepsilon) \quad \begin{cases} \frac{dx}{dt} = -\lambda y + \varepsilon x - ax(x^2+y^2) \\ \frac{dy}{dt} = \lambda x + \varepsilon y - ay(x^2+y^2) \end{cases}$$

where λ, a are some fixed constants > 0 and we are interested in x, y, ε close to 0.

For all ε we have an equilibrium at $(x = 0, y = 0)$, and the eigenvalues are $\pm i\lambda + \varepsilon$: therefore the equilibrium is stable for $\varepsilon < 0$, unstable for $\varepsilon > 0$.

Going to (modified) polar coordinates $R = (x^2 + y^2)$, $\theta = \arctan y/x$ gives

$$\begin{cases} \frac{dR}{dt} = 2(x\dot{x} + y\dot{y}) = 2R(\varepsilon - R) \\ \frac{d\theta}{dt} = \frac{x\dot{y} - y\dot{x}}{x^2+y^2} = \lambda \end{cases}$$

which can be solved explicitly: the angular velocity is constant; if $\varepsilon < 0$, all solutions converge to the equilibrium; if $\varepsilon > 0$, all solutions but the equilibrium converge to the periodic orbit

$$\begin{cases} R = \varepsilon \\ \dot{\theta} = \lambda \end{cases}$$

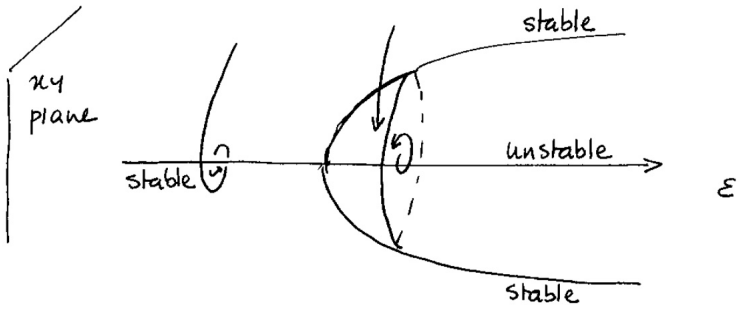

B.2. **The general phenomenon.** One considers a 1-parameter family of differential equations in $\mathbb{R}^N$

$$(*_\varepsilon) \quad \frac{dx}{dt} = F_\varepsilon(x)$$

with the following assumptions

(H0) For $\varepsilon = 0$, we have an equilibrium at $x = 0$ ($\in \mathbb{R}^N$); moreover the eigenvalues of D_0F_0 have negative real part, except two which are purely imaginary, distinct from 0 (and complex conjugate to each other); let $\mu_0 = i\lambda$ and $\overline{\mu}_0 = -i\lambda$ be these eigenvalues.

This hypothesis allows after a change of variables in the neighborhood of the equilibrium to rewrite $(*_0)$ as

$$\begin{cases} \frac{dx_0}{dt} = -\lambda x_1 - ax_0(x_0^2 + x_1^2) + h.o.t. \\ \frac{dx_1}{dt} = \lambda x_0 - ax_1(x_0^2 + x_1^2) + h.o.t. \\ \frac{dx'}{dt} = Ax' + h.o.t. \end{cases}$$

where $x = (x_0, x_1, x')$, $x' \in \mathbb{R}^{N-2}$, and the eigenvalue of the $(N-2) \times (N-2)$ matrix A have negative real part.

We next assume that

(H1) $a > 0$

The final assumption involves dependence on the parameter ε: for ε close to 0, we can follow the non-degenerate equilibrium and the eigenvalues μ_ε, $\overline{\mu}_\varepsilon$ close to the imaginary axis. One assumes that

(H2) $\frac{\partial}{\partial \varepsilon} \text{Re } \mu_\varepsilon > 0$ at $\varepsilon = 0$.

Under hypotheses (H0), (H1), (H2), the dynamics of the equations $(*_\varepsilon)$ are as in the plane model:

- for $\varepsilon < 0$, we have a stable equilibrium
- for $\varepsilon = 0$, it is still stable but weakly so;
- for $\varepsilon > 0$, the equilibrium is unstable, but we have a "circular" periodic orbit which is stable and has diameter $\sim \sqrt{\varepsilon}$.

APPENDIX C. HOPF BIFURCATION FOR PERIODIC ORBITS OR DIFFEOMORPHISMS

C.1. **Poincaré return map.** Assume that a differential equation

$$(*_0) \quad \frac{dx}{dt} = F_0(x), \quad x \in \mathbb{R}^N$$

has a periodic solution $x_0(t+T) = x_0(t)$. To study the dynamics of $(*_0)$ near this solution, Poincaré considers a transversal Σ to this orbit and introduces the first return map to Σ (see picture)

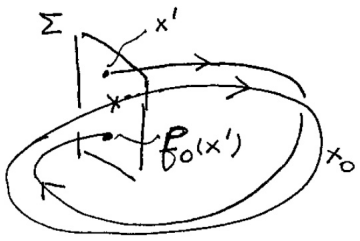

which leads to the study of a diffeomorphism f_0 near a fixed point x_0' corresponding to the periodic orbit.

If one considers a slight deformation $(*_\varepsilon)$ of $(*_0)$ one can still introduce the first return map f_ε for this new equation, and it is a slight deformation of f_0.

Thus, the study of differential equations near a periodic orbit is equivalent to that of diffeomorphisms (i.e. discrete time) near fixed points.

We will go to this context in the following.

C.2. **Model in the plane.** Identifying $\mathbb{R}^2$ to $\mathbb{C}$, we consider

$$f_\varepsilon(z) = \lambda(1+\varepsilon)z - az|z|^2$$

where $|\lambda| = 1$, $a > 0$ are fixed and ε close to 0 is a real parameter; we assume $\lambda \neq \pm 1$. We have

$$\begin{cases} |f_\varepsilon(z)| = |z|(1+\varepsilon - a|z|^2), \\ \text{Arg } f_\varepsilon(z) = \text{Arg } z + \text{Arg } \lambda \end{cases}$$

hence the fixed point $z = 0$ is stable for $\varepsilon < 0$, weakly stable for $\varepsilon = 0$, unstable for $\varepsilon > 0$; on the other hand, the circle

$$|z| = \left(\frac{\varepsilon}{a}\right)^{1/2}$$

is invariant and attracts all orbits close to 0 except the equilibrium itself when $\varepsilon > 0$.

C.3. **The general phenomenon.** One considers a 1-parameter family of diffeomorphisms

$$x \mapsto f_\varepsilon(x), \quad x \in \mathbb{R}^N.$$

One assumes that f_0 has a fixed point at 0, and that the eigenvalues of $D_0 f_0$ have modulus < 1 except two, say $\mu_0, \overline{\mu}_0$ for which $|\mu_0| = 1$.

Moreover one assumes that $\mu_0^k \neq 1$ for $k = 1, 2, 3, 4$ (i.e., $\mu_0 \neq \pm 1, \pm i, \pm j$). Then one formulates (H1'), (H2') in completely the same way that Appendix B and get the same description of the dynamics that in the plane model.

In particular, for $\varepsilon > 0$, we get a stable invariant "circular" curve of radius $\sim \varepsilon^{1/2}$.

However, the dynamics *on the curve* are not necessarily as simple as in the plane model (where it is a rigid rotation by Arg λ): what one gets is a diffeomorphism of the curve

close to a rigid rotation. This in general does *not* imply that it behaves like a rigid rotation. However, for most parameters (in the measure-theoretical sense), it can be proven that these dynamics are smoothly conjugated to a rigid (irrational) rotation.

This last case corresponds to quasiperiodic motion on a 2-dimensional torus when we started with a periodic orbit of a differential equation

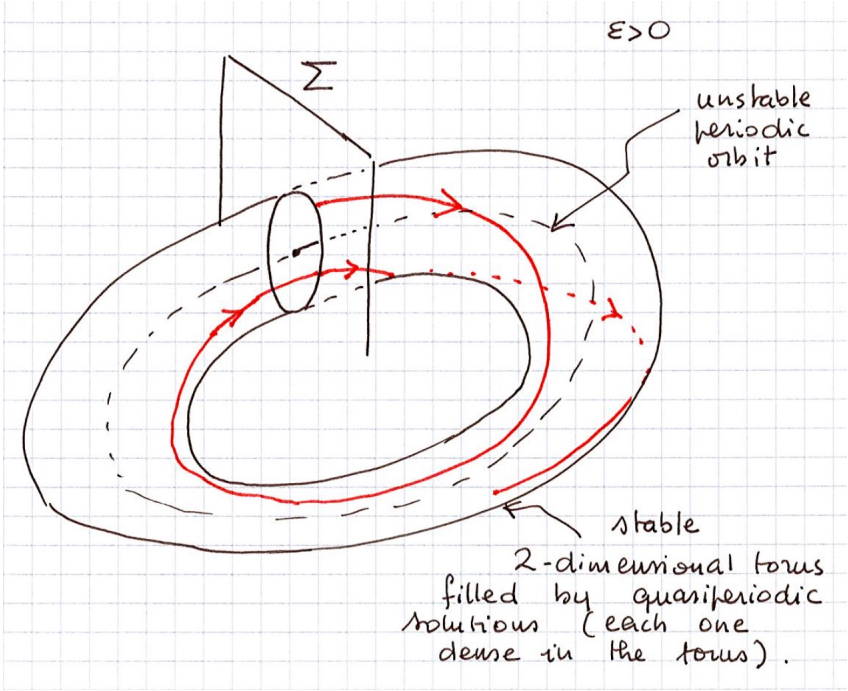

APPENDIX D. SADDLE NODES BIFURCATIONS

This is very similar (but simpler) than Hopf bifurcations.

We will deal with periodic orbits (rather than equilibria), for differential equations, and this amounts, via the Poincaré return map, to deal with fixed points of diffeomorphisms.

D.1. **The 1-D model.** Consider the 1-parameter family of local diffeomorphisms

$$f_\varepsilon(x) = x + x^2 - \varepsilon \qquad \begin{matrix} x \in \mathbb{R} \text{ close to } 0 \\ \varepsilon \text{ small} \end{matrix}$$

If $\varepsilon < 0$, we have $f_\varepsilon(x) - x = x^2 - \varepsilon > 0$, and thus no fixed points near 0 (orbits cross from left to right in a neighborhood of 0

If $\varepsilon = 0$, we have a fixed point at 0 with eigenvalue 1 which is *semi-stable*: it attracts a half-neighborhood.

If $\varepsilon > 0$, we have two fixed points $\pm\varepsilon^{1/2}$, with eigenvalues $1 \pm 2\varepsilon^{1/2}$: therefore $\varepsilon^{1/2}$ is unstable while $-\varepsilon^{1/2}$ is stable

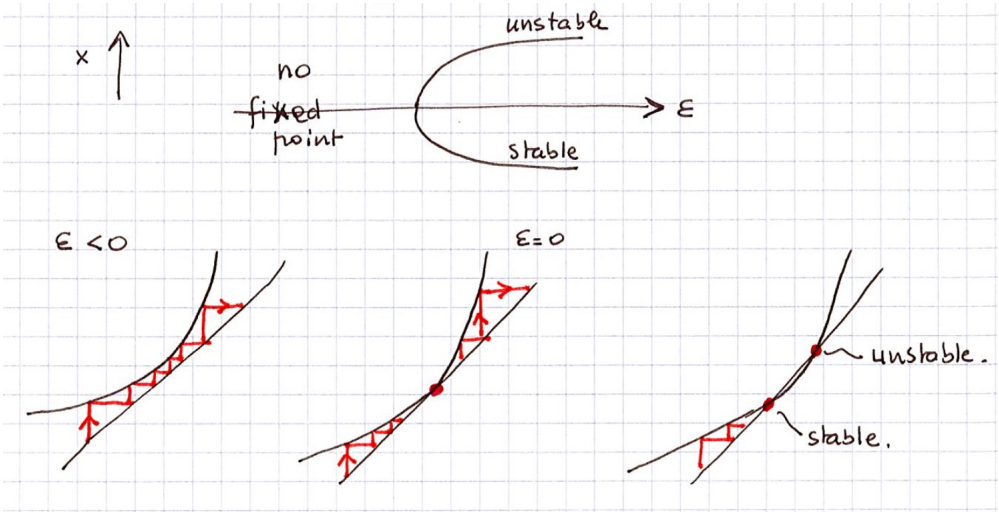

D.2. **The general phenomenon.** We have a 1-parameters family of local diffeomorphisms

$$x \mapsto f_\varepsilon(x) \qquad x \in \mathbb{R}^N, \text{ close to } 0$$

We assume that

(H0) 0 is a fixed point for f_0; all eigenvalues of $D_0 f_0$ have modulus < 1, except one which is equal to 1 (denote this eigenvalue by μ_0)

Then, after a change of coordinates, we can write $x = (x_0, x')$, $x' \in \mathbb{R}^{N-1}$ and

$$f_0(x_0, x') = (x_0 + a x_0^2 + h.o.t, Ax' + h.o.t.)$$

(where all eigenvalues of A have modulus < 1). We assume

(H1) $a \neq 0$ (and even say $a > 0$)

Finally, writing f_ε^0 for the first coordinate of f_ε, we want that

(H2) $\frac{\partial}{\partial \varepsilon} f_\varepsilon^0(0,0) < 0$ at $\varepsilon = 0$

Then

- for $\varepsilon < 0$, there is no fixed point: orbits cross a neighborhood of 0 with increasing x_0
- for $\varepsilon = 0$ there is a semistable fixed point attracting a half-neighborhood
- for $\varepsilon > 0$ there are two fixed points (at distance $\sim \varepsilon^{1/2}$): one is stable while the other is unstable (with exactly one unstable eigenvalue)

APPENDIX E. SOME CHAOTIC ATTRACTORS

We start with the simplest ones: *uniformly hyperbolic attractors*, where we describe the simplest example: the *solenoid*. Unfortunately, this class requires a geometry that does not seem to appear in our toy model. We therefore go to the larger class of *non-uniformly hyperbolic attractors*, of which the prototype is the *Henon attractor*; actually, what we observe for the second set of parameter values look very much like the Henon attractor ...!!

E.1. **Uniformly hyperbolic attractors: the solenoid.** Consider the full torus $T = \{(\theta, z), \theta \in \mathbb{R}/\mathbb{Z}, z \in \mathbb{C}, |z| \leqslant 1\}$ and the map

$$\begin{aligned} f: \quad T \quad &\to \quad T \\ (\theta, z) \quad &\to (2\theta \bmod 1, \frac{1}{2}e^{2\pi i\theta} + \frac{1}{3}z) \end{aligned}$$

(thus the map expands the θ coordinate and contracts the z-coordinate (2-dimensional)).

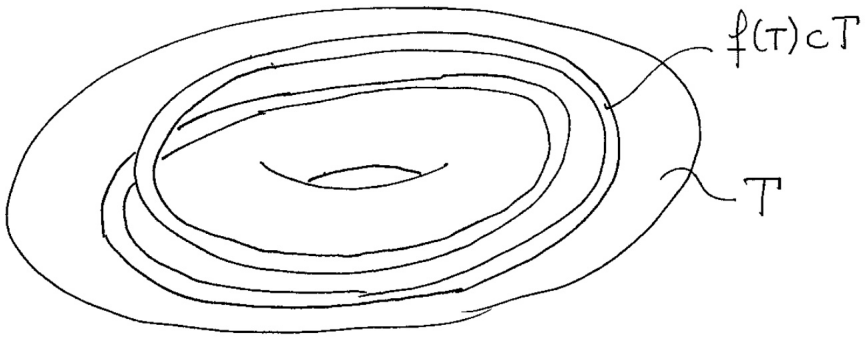

The attractor Λ is

$$\Lambda = \bigcap_{n \geqslant 0} f^n(T)$$

If we consider the intersection of Λ with any disk $\{\theta = \theta_0\}$, we get a Cantor set

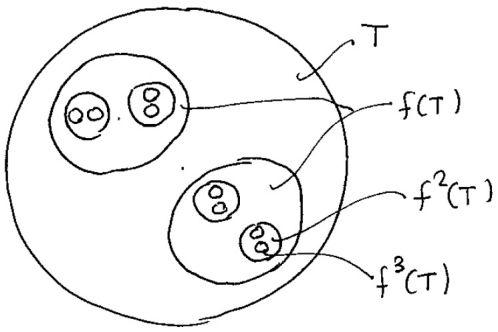

hence Λ is locally the product of a Cantor set and a line.

We now list some properties of Λ which are characteristic of hyperbolic attractors.

(1) At every point $x = (\theta, z)$ in Λ, there is a linear decomposition

$$\mathbb{R}^3 = E^s_x \oplus E^u_x$$

where E^s_x is 2-dimensional (in our case, E^s_x is the plane $z = c^{te}$) and E^u_x is 1-dimensional, tangent to Λ, such that

- the tangent map Tf leaves the decomposition invariant: $Tf(E^s_x) = E^s_{f(x)}, Tf(E^u_x) = E^u_{f(x)}$
- The tangent map Tf contracts uniformly vectors in E^s_x, and expands uniformly vector in E^u_x
- E^s_x and E^u_x depend continuously on $x \in \Lambda$.

[we actually just gave the *definition* of a hyperbolic set].

(2) Sensibility w.r.t. initial conditions

Let $x = (\theta, z)$, $x' = (\theta', z')$ two points in Λ, which could be arbitrarily close; unless $\theta = \theta'$, the distance between $f^n(x)$ and $f^n(x')$ will grow [the difference of θ coordinates being multiplied by 2] till it has size ~ 1.

(3) *Shadowing property*

Consider an ε pseudo-orbit, i.e. a sequence $(x_n)_{n\geqslant 0}$ near Λ with

$$d(x_{n+1}, f(x_n)) < \varepsilon$$

Then, there exists a *true* orbit $(f^n x)_{n\geqslant 0}$ s.t.

$$d(x_n, f^n x) < C\varepsilon$$

Remark E.1. This is fundamental: indeed, because of roundoff errors, any numerical simulation leads to pseudoorbits; the shadowing property guarantees that what we see on the screen actually happens in the attractor (but probably not *exactly* for the given initial condition).

(4) *Structural stability*

This is closely related to the shadowing property.

Assume that we perturb our map f to some nearby map g; define

$$\Lambda_g = \bigcap_{n\geqslant 0} g^n(T)$$

Then there is a homeomorphism h from Λ onto Λ_g which conjugates f on Λ and g on Λ_g:

$$h \circ f = g \circ h$$

In other terms, up to a continuous change of coordinates, *we see exactly the same picture and dynamics for f and g.*

(5) *Physical (or Sinai–Ruelle–Bowen) measure*

There is a measure $\mu = \mu_f$ on Λ with the following property. Let φ be a continuous function on T. Pick a point x "at random" in T. Then, with probability 1 (in x), the time averages

$$\frac{1}{n}\sum_0^{n-1} \varphi(f^i x)$$

will converge to the "spatial" average

$$\int_\Lambda \varphi \, d\mu_f$$

[this is *not* the classical Boltzmann hypothesis: the measure μ is quite singular, concentrated on the attractor which has volume 0].

Moreover, the measure μ is *stochastically stable* in the following sense:

Consider a pseudoorbit $(x_n)_{n\geqslant 0}$, as above, but assume now that the ε-jumps from $f(x_n)$ to x_{n+1} are independent random variables.

Then the time averages

$$\frac{1}{n}\sum_0^{n-1}\varphi(x_i)$$

will converge, as $n\to+\infty$ and then $\varepsilon\to 0$, to $\int_\Lambda \varphi\, d\mu_f$.

Remark E.2. It is not quite true that the roundoff errors in numerical simulation are independent random variables! Still, due to the sensibility to initial conditions, there is some degree of independence, and it is reasonable to expect that the points we compute will "charge" Λ according to μ_f.

E.2. **Non-uniformly hyperbolic attractors: the Henon attractor.** We consider the map $H = H_{b,c} : \mathbb{R}^2 \to \mathbb{R}^2$

$$\begin{pmatrix} x \\ y \end{pmatrix} \to \begin{pmatrix} x^2 + c - by \\ x \end{pmatrix}$$

where $0 < b \ll 1$ and c is slightly larger than -2. There is a rectangle R for which the picture looks like

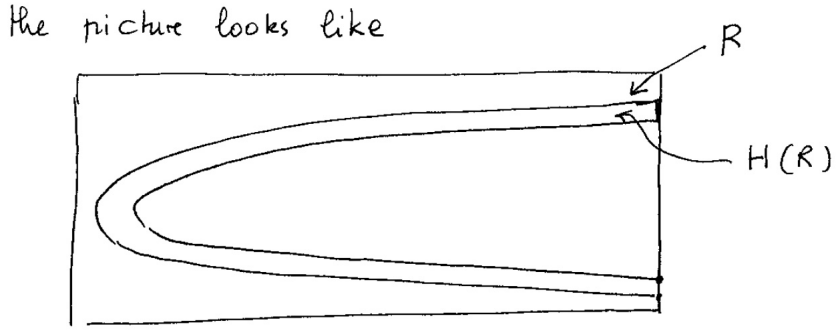

[the rectangle is *strectched* and *folded*; for the solenoid, there is only a *stretching*; all the complications in the present case come from the *fold*]

The attractor Λ is now

$$\Lambda = \bigcap_{n\geqslant 0} H^n(R)$$

At a *typical point of* Λ, a zoom will give

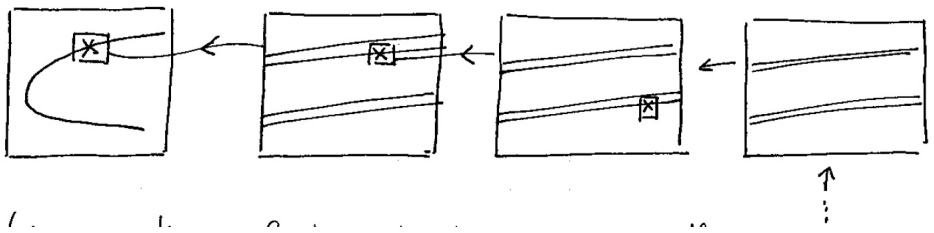

(i.e. a line $\times$ Cantor structure, as was the case at *all* points in the solenoid), but there are some *nasty* points (dense in Λ) where the zoom is rather like

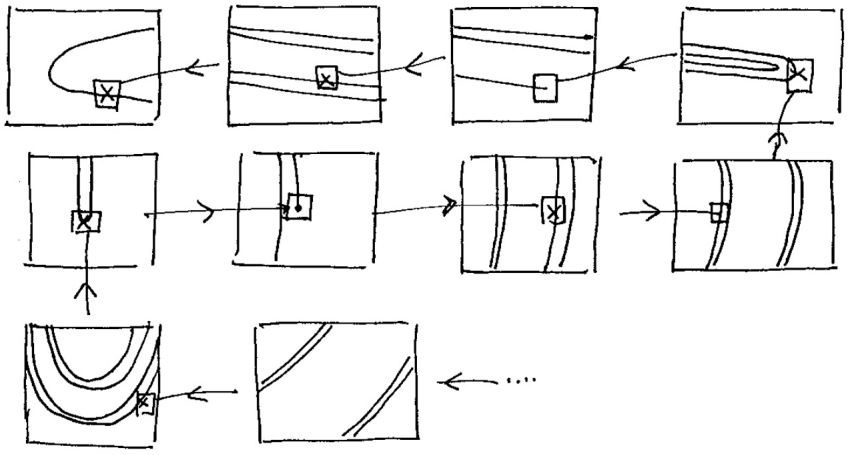

For *most* (but not *all*) values of parameter c, the properties of Λ are the following:

(1) the decomposition

$$\mathbb{R}^2 = E^s_x \oplus E^u_x$$

is only valid at almost all points (w.r. to the physical measure, see (5) below), but E^s_x, E^u_x now do not depend continuously on x, and the contraction and expansion are *not* uniform in x

(2) Sensibility w.r. to initial conditions still holds.

(3) The shadowing property holds for most pseudoorbits, but there are some (*very special*) pseudoorbits which are not approximated by true orbits.

(4) Structural stability *does not hold* [actually, with arbitrarily small perturbations of c, we can get completely different dynamics]. Still, for *most* perturbations of $H_{b,c}$, we get an attractor of the same kind.

(5) Physical measure.

This still exists and has the same properties (stochastic stability) than for the solenoid.

Commentary: The theory of hyperbolic attractors was completed by $\sim$ 1970. For non-uniformly hyperbolic ones, the theory is *far from complete*, and it is a "hot" subject at the moment.

E.3. **Possible geometries of the chaotic attractors E.1, E.2.** (E.2) looks very much like a Henon attractor

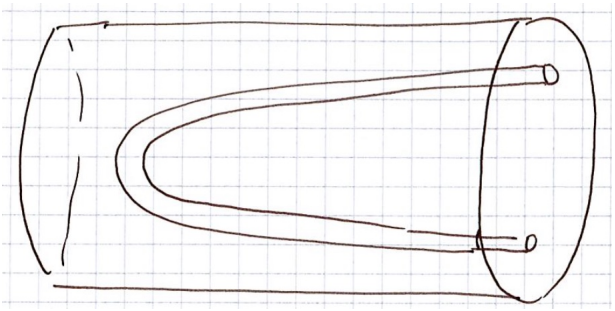

A tube is *stretched* and *folded* inside itself.

The transverse contraction (∞-dimensional!) should be *stronger* than the strectching.

in (E.1), the geometry could (!?!?) be as follows with more complicated strectching and folding.

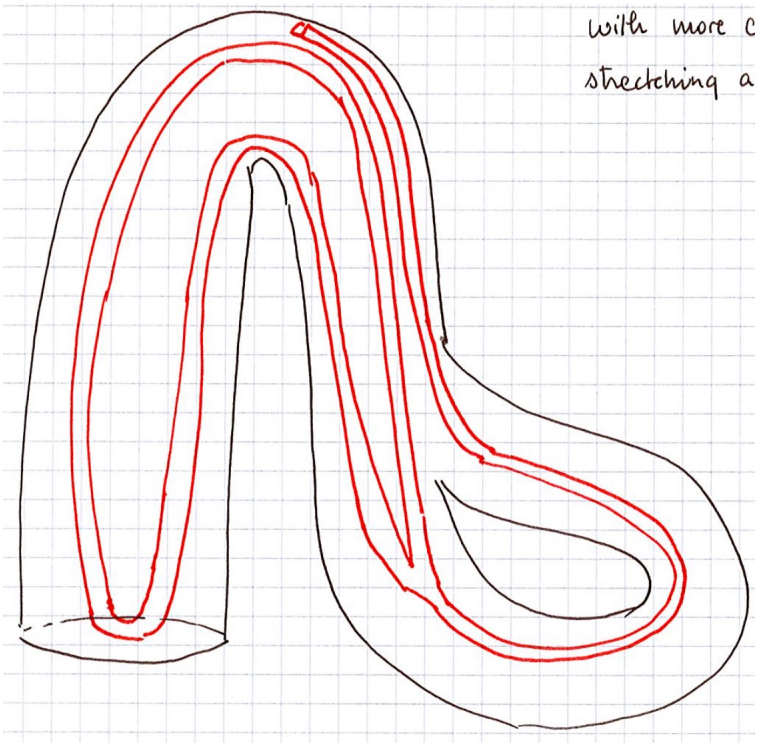

APPENDIX F. A PRIORI ESTIMATES IN THE TOY MODEL

Let $t_0 \in \mathbb{R}/\mathbb{Z}$ and N an element of Y_{t_0}, i.e. a continuous function on $[-A_1, 0]$ which satisfies

$$N(0) = \int_{A_0}^{A_1} S(a)N(-a)m(N(-a))m_\rho(t_0 - a)\, da,$$

and takes only positive values. For $0 \leqslant s \leqslant A_0$, we define

$$\overline{N}(s) = \int_{A_0}^{A_1} S(a)N(s-a)m(N(s-a))m_\rho(t_0 + s - a)\, da,$$

(we have $\overline{N}(0) = N(0)$, hence $\overline{N}$ extends N and gives a solution of the toy model). *We assume always* $\gamma \geqslant 1$.

Lemma F.1. *For any* $N \in Y_{t_0}$ *we have, for* $0 \leqslant s \leqslant A_0$

$$\overline{N}(s) \leqslant N_{\max} = m_0 \frac{A_1}{2}(1 - \frac{A_0}{A_1})^2$$

Proof. We have

$$Nm(N) = \begin{cases} m_0 N & \text{if } N \leqslant 1 \\ m_0 N^{1-\gamma} & \text{if } N \geqslant 1 \end{cases}$$

hence $Nm(N) \leqslant m_0$ in all cases. Therefore, as $m_\rho \leqslant 1$

$$\overline{N}(s) \leqslant m_0 \int_{A_0}^{A_1} S(a)\, da = N_{\max}$$

□

We introduce the quantity

$$c_0 = \int_{A_0+\rho}^{A_0+1} S(a)\, da = (1-\rho)\left(1 - \frac{A_0 + \frac{1+\rho}{2}}{A_1}\right)$$

We will always assume $c_0 m_0 > 1$.

Lemma F.2. *Let* $N \in Y_{t_0}$ *satisfying* $N \leqslant N_{\max}$*; define*

$$i(N) = \min(N(-a), 0 \leqslant a \leqslant A_1) > 0$$

If $i(N) \leqslant N_{\max}^{1-\gamma}$ *we have*

$$\overline{N}(s) \geqslant c_0 m_0 i(N) (> i(N)) \quad \textit{for all } 0 \leqslant s \leqslant A_0$$

If $i(N) \geqslant N_{\max}^{1-\gamma}$ *we have*

$$\overline{N}(s) \geqslant c_0 m_0 N_{\max}^{1-\gamma} \quad \textit{for all } 0 \leqslant s \leqslant A_0$$

Corollary F.3. *If* $\gamma \geqslant 1$, $c_0 m_0 > 1$, *any solution* $N(t)$ $(-A_1 \leqslant t < +\infty)$ *of the toy model satisfies*

$$c_0 m_0 N_{\max}^{1-\gamma} \leqslant N(t) \leqslant N_{\max}$$

for t *large enough.*

Proof of Lemma F.2. We have now, for $i(N) \leqslant N \leqslant N_{\max}$

$$\begin{aligned} Nm(N) &\geqslant m_0 N_{\max}^{1-\gamma} \quad \text{if } i(N) \geqslant N_{\max}^{1-\gamma}, \\ &\geqslant m_0 i(N) \quad \text{if } i(N) \leqslant N_{\max}^{1-\gamma} < 1, \end{aligned}$$

and therefore

$$\overline{N}(s) \geqslant m_0 \inf(i(N), N_{\max}^{1-\gamma}) \int_{A_0}^{A_1} S(a) m_\rho(t_0 + s - a)\, da$$

It is now easy to check that, as S is decreasing, we have, for any $u \in \mathbb{R}$

$$\int_{A_0}^{A_1} S(a) m_\rho(u - a)\, da \geqslant \int_{A_0+\rho}^{A_0+1} S(a)\, da = c_0$$

This gives lemma F.2. □

Lemma F.4. *Let $N \in Y_{t_0}$, satisfying $N \leqslant N_{\max}$; define*

$$L = m_0(2 - \frac{A_0}{A_1}).$$

For $0 \leqslant s_0, s_1 \leqslant A_0$, we have

$$|\overline{N}(s_0) - \overline{N}(s_1)| \leqslant L|s_0 - s_1|.$$

Proof. We have

$$\overline{N}(s_i) = \int_{s_i - A_1}^{s_i - A_0} S(s_i - u) N(u) m(N(u)) m_\rho(t_0 + u)\, du$$

Here we have $N(u)m(N(u)) \leqslant m_0$ and $m_\rho(t_0 + u) \leqslant 1$; moreover $0 \leqslant S(s_i - u) \leqslant 1$ and

$$|S(s_1 - u) - S(s_0 - u)| \leqslant A_1^{-1}|s_1 - s_0|$$

Therefore

$$\begin{aligned} |\overline{N}(s_1) - \overline{N}(s_0)| &= |\int_{s_0 - A_1}^{s_0 - A_0} [S(s_1 - u) - S(s_0 - u)] N(u) m(N(u)) m_\rho(t_0 + u)\, du \\ &+ \int_{s_0 - A_0}^{s_1 - A_0} - \int_{s_0 - A-1}^{s_1 - A_1} S(s_1 - u) N(u) m(N(u)) m_\rho(t_0 + u) du| \\ &\leqslant m_0(1 - \frac{A_0}{A_1})|s_0 - s_1| + m_0|s_0 - s_1| \\ &\leqslant L|s_0 - s_1| \end{aligned}$$

□

We now introduce

$$\begin{aligned} \mathcal{K}_{t_0} = \{&N \in Y_{t_0}, \text{ for any } s \in [-A_1, 0] \\ &c_0 m_0 N_{\max}^{1-\gamma} \leqslant N(s) \leqslant N_{\max} \text{ and for any} \\ &s_0, s_1 \in [-A_1, 0], |N(s_0) - N(s_1)| \leqslant L|s_0 - s_1|\} \end{aligned}$$

A basic theorem in elementary analysis (Ascoli's theorem) guarantees that $\mathcal{K}_{t_0}$ is a *compact* subset of Y_{t_0} (for the uniform convergence topology).

The lemmas above prove the following

Proposition F.5. *Let $N \in Y_0$; write*

$$T^s(0, N) = (s \bmod 1, N^s) \quad \text{for all } s \geqslant 0$$

a) If $N \in \mathcal{K}_0$, then $N^s \in \mathcal{K}_s$ for all $s \geqslant 0$; in particular, $T^1(\mathcal{K}_0) \subset \mathcal{K}_0$.
b) In any case, there exists s_0 such that $N^s \in \mathcal{K}_s$ for all $s \geqslant s_0$.

The *attractor* of the toy model is then defined as

$$\Lambda = \{(t, N), t \in \mathbb{R}/\mathbb{Z}, N \in \Lambda_t\}$$

where

$$\Lambda_t = \bigcap_{n \geqslant 0} T^n(\mathcal{K}_t)$$

We have

$$T^s(\Lambda_t) = \Lambda_{t+s}$$

and in particular

$$T^1(\Lambda_0) = \Lambda_0.$$

The set Λ, Λ_t are *compact*; the set Λ satisfies:

for any neighborhood U of Λ, and any initial condition $(0, N)$ ($N \in Y_0$), there exists $s_0 = s_0(N, U)$ such that

$$T^s(0, N) \in U \quad \text{for all } s \geqslant s_0$$

(which explains the terminology attractor).